BIOCHEMISTRY
including biophysical chemistry & molecular biology

Article

pubs.acs.org/biochemistry

Hydrogen Exchange Mass Spectrometry of Functional Membrane-Bound Chemotaxis Receptor Complexes

Seena S. Koshy,[†] Stephen J. Eyles,[‡] Robert M. Weis,[†,§,∥] and Lynmarie K. Thompson*[,†,§]

[†]Department of Chemistry, [‡]Department of Biochemistry and Molecular Biology, and [§]Program in Molecular and Cellular Biology, University of Massachusetts, Amherst, Massachusetts 01003, United States

Supporting Information

ABSTRACT: The transmembrane signaling mechanism of bacterial chemotaxis receptors is thought to involve changes in receptor conformation and dynamics. The receptors function in ternary complexes with two other proteins, CheA and CheW, that form extended membrane-bound arrays. Previous studies have shown that attractant binding induces a small (~2 Å) piston displacement of one helix of the periplasmic and transmembrane domains toward the cytoplasm, but it is not clear how this signal propagates through the cytoplasmic domain to control the kinase activity of the CheA bound at the membrane-distal tip, nearly 200 Å away. The cytoplasmic domain has been shown to be highly dynamic, which raises the question of how a small piston motion could propagate through a dynamic domain to control CheA kinase activity. To address this, we have developed a method for measuring dynamics of the receptor cytoplasmic fragment (CF) in functional complexes with CheA and CheW. Hydrogen−deuterium exchange mass spectrometry (HDX-MS) measurements of global exchange of the CF demonstrate that the CF exhibits significantly slower exchange in functional complexes than in solution. Because the exchange rates in functional complexes are comparable to those of other proteins with similar structures, the CF appears to be a well-structured protein within these complexes, which is compatible with its role in propagating a signal that appears to be a tiny conformational change in the periplasmic and transmembrane domains of the receptor. We also demonstrate the feasibility of this protocol for local exchange measurements by incorporating a pepsin digest step to produce peptides with 87% sequence coverage and only 20% back exchange. This method extends HDX-MS to membrane-bound functional complexes without detergents that may perturb the stability or structure of the system.

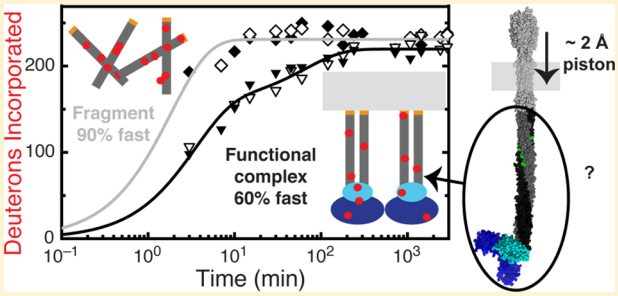

Membrane proteins and their complexes are involved in many life processes, including signal transduction, energy transduction, transmembrane transport, cell adhesion, and cell motility. Our mechanistic understanding of these processes is hampered by the challenging nature of studies of membrane proteins. There is very limited structural information on membrane proteins, which comprise <2% of known structures in the Protein Data Bank, and the methods for investigating mechanistic roles of dynamics have been historically difficult to extend to membrane proteins.

There has been recent success in measuring functionally important dynamics in membrane proteins. Solution nuclear magnetic resonance (NMR), for example, which has provided key insights into the role of dynamics in catalysis by soluble proteins,[1] has recently been used to measure the effects of ligands on conformational equilibria between inactive and activated states of the detergent-solubilized β2-adrenergic receptor, providing insight into different types of activation.[2−4] Unfortunately, such approaches are difficult to apply to a high-molecular weight system, such as a membrane protein in a more native lipid bilayer environment or in a large complex with additional proteins, because slow tumbling causes severe resonance broadening.

Although mass spectrometry does not have this limitation regarding molecular weight, membrane proteins and their complexes have long been assumed to be too challenging a target for MS, for example, because of ionization suppression caused by some detergents.[5−7] There has been remarkable recent progress in this area: multiple large membrane protein complexes have been analyzed by MS to reveal subunit stoichiometry and native lipid interactions.[8,9] Hydrogen−deuterium exchange mass spectrometry (HDX-MS) is a powerful approach for measuring protein dynamics, because amide proton exchange rates are sensitive to hydrogen bonding and solvent exposure.[10−12] HDX-MS has been successfully applied to a wide range of soluble proteins to measure, for example, changes resulting from mutations, ligand binding, and protein−protein interactions[13−16] as well as protein folding.[17] Recently, HDX-MS has also been used to monitor structure and dynamics in a number of detergent-solubilized membrane proteins, including G-protein-coupled receptors and their complexes,[18−20] an ADP/ATP carrier,[21] and an ABC transporter,[22] as well as in

Received: September 12, 2013
Revised: November 5, 2013
Published: November 6, 2013

dx.doi.org/10.1021/bi401261b | *Biochemistry* 2013, 52, 8833−8842

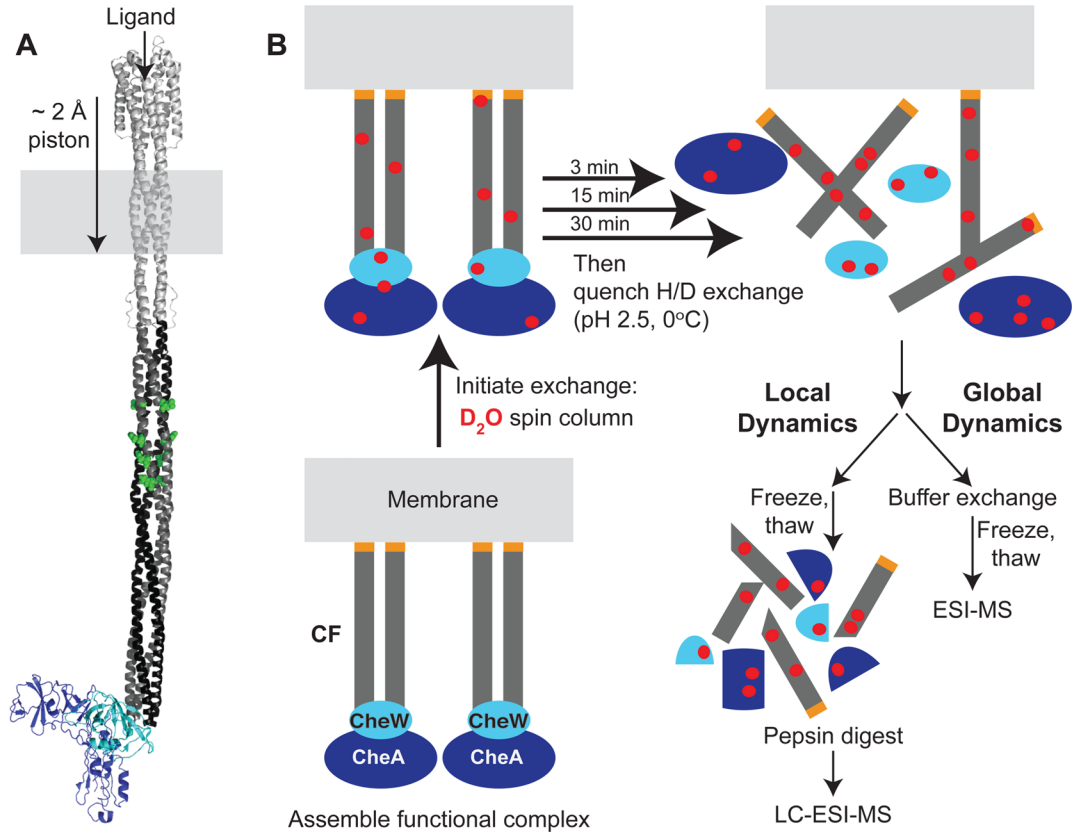

Figure 1. Method for the HDX-MS study of functional membrane-bound multiprotein complexes. (A) Model of an intact chemotaxis receptor with CheW (cyan) and CheA (blue) bound to the membrane-distal tip of the receptor cytoplasmic domain. The dimeric cytoplasmic fragment is colored black and dark gray, with the methylation sites colored green. (B) Such a membrane protein system can be simplified by assembling functional complexes on vesicles containing nickel-chelating lipids that bind the His tag (orange) of the Asp receptor cytoplasmic fragment (CF), which in turn binds the other proteins of the complex (CheA and CheW).[31] Deuterium exchange is initiated with a spin column to avoid dilution and dissociation of the complex. Exchange is quenched by lowering the temperature and pH. For global HDX measurements, the buffer is exchanged using spin columns and samples are flash-frozen and stored until they are analyzed by ESI-MS. For local HDX measurements, the quenched samples are flash-frozen. Samples are later thawed, digested with pepsin, injected onto a C18 column, and analyzed by LC-ESI-MS.

a nanodisc-inserted membrane protein.[23] Thus, HDX-MS is a promising tool for measuring functional dynamics of membrane proteins.

Bacterial chemotaxis receptors, which have been widely studied in an effort to understand the detailed mechanism of transmembrane signaling, display a paradoxically dynamic cytoplasmic domain.[24,25] These receptors (Figure 1A) bind ligands in the periplasm and transmit a signal that controls activation of a kinase bound to the cytoplasmic tip of the receptor. Within the periplasmic and transmembrane regions, the ligand-induced signal is widely believed to consist of a tiny (~2 Å) piston motion of a transmembrane helix toward the cytoplasm.[26] However, the cytoplasmic domain is known to be highly dynamic: a cytoplasmic fragment (CF) exchanges 90% of its amide protons with deuterium within 10 min,[24] and the cytoplasmic domain of the intact receptor exhibits promiscuous cysteine cross-linking.[25,27] How could a 2 Å piston motion be coupled through a dynamic cytoplasmic domain to control activation of the associated kinase? Chemotaxis receptors are known to operate in bacteria in large arrays (dimensions of ~200 nm) consisting of receptors and the associated CheW and CheA proteins,[28−30] so perhaps the cytoplasmic domain dynamics are reduced in these complexes. Measurements of receptor dynamics in functional complexes are needed to resolve this paradox.

To study receptor dynamics in nativelike arrays, we sought to avoid detergent solubilization that often perturbs the stability and function of membrane proteins. We developed an alternate approach that combines "template-directed assembly"[31] with HDX-MS for measuring dynamics in functional protein complexes bound to membrane vesicles. Template-directed assembly[32] was developed by Weis and co-workers to assemble functional complexes of the CF of the aspartate receptor with CheA and CheW. The method employs vesicles containing a nickel-chelating lipid that binds to a histidine-tagged fragment of a membrane protein (CF), to which the other proteins bind to assemble a functional complex. This restores kinase activation that is lost in detergent-solubilized receptor preparations. Furthermore, both the kinase-activating (kinase-on) and methylation-activating (kinase-off) signaling states of the system can be produced by controlling the receptor density on the vesicles.[33]

The combined template-directed assembly HDX-MS method for measurement of dynamics in functional, membrane-bound multiprotein complexes in shown in Figure 1B. This approach is used for global exchange measurements on the Asp chemotaxis receptor CF, which demonstrate that formation of functional complexes significantly reduces its dynamics. Furthermore, we show that the method is compatible with local exchange measurements by identifying pepsin digest products

dx.doi.org/10.1021/bi401261b | *Biochemistry* 2013, 52, 8833−8842

covering 87% of the CF sequence, which will allow future measurements to test proposed models for how dynamics change during signaling.[34,35] Because other membrane protein systems are amenable to template-directed assembly,[36−39] this provides a general HDX-MS approach for measuring functionally important dynamics in membrane protein complexes bound to vesicles, complementary to current applications of HDX-MS to membrane proteins in detergent micelles or nanodiscs.

MATERIALS AND METHODS

Preparation and Characterization of Signaling Complexes. CheA, CheW, CheY, and the CF were prepared using published protocols.[40−43] Functional complexes of the CF, CheA, and CheW bound to vesicles were prepared as previously described,[33] using excess CheA and CheW to drive incorporation of all of the CF into complexes.[42] These complexes were characterized using kinase and sedimentation assays.[31] Details of these protocols are described in the Supporting Information.

Global HDX-MS Measurements. Spin columns were used both to initiate hydrogen exchange and to transfer samples into MS-compatible buffers. Unless otherwise specified, all centrifugation steps consisted of 2 min spins at 2000 rpm in a Beckman Coulter Allegra 6R Tabletop Centrifuge, at the specified temperatures. Hydrogen exchange was initiated using a 5 mL G10 Sephadex Zeba desalting column (Pierce Biotechnology), pre-equilibrated by four spins at 25 °C, each with a 2 mL aliquot of D_2O kinase buffer [75 mM Tris, 100 mM KCl, 5 mM $MgCl_2$, 2 mM TCEP, and 5% DMSO (pH electrode reading of 7.1, corresponding to a pD_{corr} of 7.5)]. For the buffer exchange step, columns were prepared by hydrating 5 g of G25 Sephadex beads (Sigma-Aldrich) overnight in 25 mL of water to obtain a suspension of swollen beads (sufficient for approximately thirty 1 mL columns). The next day, for each 1 mL syringe column, cotton wool was placed in the bottom of the syringe, the overnight hydrated G25 bead suspension was transferred onto the upright standing syringe to yield a volume of 1 mL, and the water was allowed to drain completely. The column was equilibrated with 2 mL of desalting buffer [20 mM ammonium formate (pH 2.5) and 10% acetonitrile] in sequential 200 μL aliquots, and the solvent was allowed to drain through the column by gravity. To prevent the column from drying, 200 μL of the desalting buffer was added to the closed column, which was then sealed with parafilm and kept on ice for use later in the day. Just before being used, the excess solvent was removed from each desalting column by centrifugation at 4 °C.

The preparation of the exchanged samples began with assembly of 2.5 mL of the relevant complex, which was checked for kinase activity, protein binding, and protein dissociation upon quenching, as described above. To initiate deuterium exchange, 2.0 mL of functional complexes was added to the 5 mL exchange column pre-equilibrated with room-temperature D_2O kinase buffer, and the column was immediately centrifuged at 4 °C. After the approximately 0.5 min deceleration of the centrifuge, the eluted exchanged complex was immediately placed in a 25 °C water bath. For each time point, 100 μL of the exchanged complex was removed and exchange was quenched by addition of 10 μL of prechilled 50 mM potassium phosphate buffer (pH 1.1), bringing the final pH to 2.5. The quenched complex was immediately transferred to a prechilled desalting column and spun at 1000 rpm for 1 min at 4 °C for exchange with a MS-compatible buffer [20 mM ammonium formate (pH 2.5) and 10% acetonitrile]. The flow through was transferred to a prechilled 1.5 mL Eppendorf tube, flash-frozen in liquid nitrogen, and stored at −80 °C until further analysis. Just before MS analysis, the sample was thawed in a 0 °C ice/water bath for 3 min.

Note that deuterium exchange occurred primarily at 25 °C (except as noted below) and all postquench steps were conducted at 0−4 °C. The centrifugation of the exchange column was conducted in a 4 °C centrifuge because of the need to immediately desalt the first quenched sample at this temperature. Thus, the first 2.5 min of exchange for all time points occurred between room temperature and 4 °C, the temperatures of the exchange column and centrifuge, respectively.

Mass spectrometry was performed on an Esquire electrospray ion trap mass spectrometer (Bruker Daltonics) at the University of Massachusetts Mass Spectrometry Center. Before analysis, the performance of the instrument was checked by injection of a 10 μM cytochrome *c* (Sigma Aldrich) control sample, and then the line was cleaned thoroughly with three injections of 100 μL of desalting buffer. Sample injections were conducted with a flow rate of 120 μL/h. The source spray parameters were optimized for the lowest possible temperature to minimize back exchange, by increasing dry gas and nebulizer values to maintain good MS signals (dry temperature of 150 °C, dry gas at 10 L/min, and nebulizer at 20.00 psi). MS experiments were conducted in positive ion mode, and spectra were obtained from m/z 1100 to 1550 over a 1 min acquisition period.

Bruker Daltonics Data Analysis software was used to convert the raw data to an average mass spectrum containing the series of m/z values for the protein. Data were processed with a smoothing value of 0.5 and a baseline subtraction of 0.8 to obtain symmetrical peaks with a good signal-to-noise ratio and deconvoluted to obtain the average molecular weight (MW) of the protein. The number of protons exchanged for deuterons at each time point was determined by subtracting the MW of the unexchanged protein from the MW of the exchanged protein. The number of exchanged protons was plotted versus time and fit to monoexponential ($y = f_1 - f_1e^{k_1t}$) and biexponential [$y = f_1 + f_2 - (f_1e^{k_1t} + f_2e^{k_2t})$] curves using ProFit (Quantum Soft).

Two methods were used to determine the number of backbone amide protons that underwent back exchange to deuterium following the quench step into protonated buffers. In the first method, two 100 μL control samples of the nonexchanged soluble CF were each quenched with a 10 μL aliquot of 50 mM potassium phosphate buffer in D_2O buffer (pD 1.4); one sample was loaded on a column previously equilibrated with 4 °C H_2O desalting buffer, and the other was loaded on a column previously equilibrated with 4 °C D_2O desalting buffer. The same control experiment was conducted on two samples of the CF in functional complexes. Subsequent steps were identical to the handling of quenched experimental samples, so differences in deuterium incorporation in each sample pair should correspond to the extent of postquench exchange that occurred under our experimental conditions. The second method involved preparation of a fully exchanged sample by denaturation of the CF in D_2O. Although the CF has previously been shown to be reversibly denatured,[44] protein aggregation was observed when CF_{4E} was heated to 80 °C in kinase buffer. Therefore, 30 μM soluble CF_{4E} was first exchanged into a buffer previously shown to support reversible thermal denaturation,[45] using a 2 mL G10 Sephadex Zeba desalting column (Pierce Biotechnology) pre-equilibrated with

dx.doi.org/10.1021/bi401261b | *Biochemistry* 2013, 52, 8833−8842

a D_2O buffer containing 20 mM potassium phosphate (pD 7.5), 50 mM NaCl, and 5% DMSO. Following this spin column, the sample was heated at 80 °C for 1 h, cooled on ice for 30 min, quenched with 10 μL of potassium phosphate buffer in D_2O (pD 1.4), and applied to a column previously equilibrated with 4 °C H_2O desalting buffer. Subsequent steps were equivalent to the handling of quenched experimental samples, so the extent of proton incorporation in this fully deuterated sample should correspond to the extent of postquench exchange that occurs under our experimental conditions.

Tandem MS Identification of Peptides. Because peptides produced for the CF in solution and in functional complexes were the same, tandem MS was conducted only on the CF in solution. A 30 μL volume of 30 μM CF was quenched with 15 μL of the quench buffer used for the local exchange experiments and digested by addition of 5 μL of 200 μM porcine pepsin (giving a 1:1 enzyme:protein ratio) for 1 min in a 0 °C ice/water bath. The digest was injected at a rate of 200 μL/min into the C18 reversed phase column used for the local exchange experiments, which had been pre-equilibrated with buffer A (0.1% formic acid in water) for 10 min. Peptides were eluted directly into the MS instrument with a 30 min linear gradient from 0 to 95% buffer B (0.1% formic acid in acetonitrile) at a rate of 100 μL/min. All of the peptides eluted with 60% buffer B, but the standard 0 to 95% gradient used for most soluble proteins was used for this CF sample because no lipids were present. The strategy used for manual sequencing, aided by Analyst software, is described in the Supporting Information, and the identified peptides are listed in Table S1 of the Supporting Information.

Local HDX-MS Measurements. The preparation of the exchanged samples was similar to that used for the global exchange experiments described above, with the following exceptions. A smaller amount (1 mL) of the relevant CF complexes was prepared and tested for activity and binding, and 700 μL was applied to a smaller (2 mL) exchange column that was pre-equilibrated and centrifuged at 25 °C. For each time point, 30 μL of the exchanged complex was removed and added to 15 μL of the quench buffer [1% formic acid, 1 M GuHCl, and 20% glycerol (pH 1.6)] in a 0 °C ice/water bath, yielding a final pH of 2.5. Each sample was immediately flash-frozen in liquid nitrogen and stored at −80 °C until further analysis. Immediately prior to the MS experiment, the sample was thawed for 3 min in a 0 °C ice/water bath, porcine pepsin (Sigma-Aldrich) was added in a 1:1 protein:enzyme molar ratio, and proteolysis proceeded for 1 min at 0 °C. Subsequent injection into the HPLC column produced both desalting of the sample and separation of the peptides.

To minimize back exchange, the injector, sample loops, HPLC columns, and lines connected from both the LC pump (Agilent, model 1100 G1312A) and the mass spectrometer were immersed in ice.[46] The peptides were injected at a rate of 200 μL/min into a 2.1 mm × 5 cm C18 reverse phase column (Higgins Analytical), pre-equilibrated in 95% buffer A (0.1% formic acid in water). The sample was eluted directly into the mass spectrometer with a 5 to 40% gradient of buffer B (0.1% formic acid in acetonitrile) over 4 min, followed by 2 min at 40% and 1 min at 60% buffer B. The 60% buffer B maximum was chosen because this is sufficient to elute all the peptide but avoids elution of the lipids (which elute at 80% buffer B) into the MS instrument. The column was then re-equilibrated with 95% buffer A for 8 min in preparation for the next sample.

After each sample injection, the syringe and injector valves were flushed with 500 μL of kinase buffer, and a blank sample was injected to make sure that there were no carryover peptides from the previous run.[47] After five sample injections, the column was removed from the ESI-MS system and washed extensively for 30 min with 100% buffer B to remove the lipids that accumulated in the column during previous sample injections.

Mass spectrometry was performed on a QSTAR-XL hybrid quadrupole/time-of-flight mass spectrometer (AB SCIEX) at the University of Massachusetts Mass Spectrometry Center. Prior to MS analysis, the instrument was calibrated by direct injection of 30 μL of 10 μM renin substrate peptide (R-8129, Sigma-Aldrich), which should yield a spectrum consisting of two peaks, with monoisotopic m/z 586.9828 (+3 charge state) and 879.9703 (+2). In addition, prior to MS of exchanged CF samples, a CF_{4E} pepsin digest was injected as a control to check the performance of the column and MS. The MS instrument was set to positive ion mode, and the peptides were ionized with turbo ion spray ionization [ion source GS1 = 30 psi and GS2 = 20 psi, curtain gas at 30 psi, ion spray voltage (IS) of 4500 V, and heater temperature of 0 °C]. A 15 min gradient elution was used for peptide separation for the exchanged samples, to minimize back exchange of backbone amide protons, but the same peptides were identified on the basis of the m/z values and elution order.

RESULTS

Template-Directed Assembly HDX-MS Method for Functional Membrane-Bound Multiprotein Complexes. With the goal of probing structure and dynamics in a functional complex of chemotaxis proteins, we combined the "template-directed assembly" method developed by Weis and coworkers[31] with HDX-MS. As shown in Figure 1B, the method begins with the assembly of a membrane-bound complex of the Asp receptor CF, CheA, and CheW. Assembly of the complex on vesicles involves using a cytoplasmic fragment of a membrane protein bearing a histidine tag, in this case the Asp receptor cytoplasmic fragment, that will bind to vesicles containing a nickel-chelating lipid, DGS-NTA-Ni^{2+}. CheW and CheA bind to the cytoplasmic fragment assembled on vesicles to produce active complexes. This template-directed assembly approach can be used in general to create functional complexes of a membrane protein with its partners, as demonstrated by its successful implementation for chemotaxis receptors,[31,41] and for several eukaryotic receptor tyrosine kinases.[36−39]

Initiation of hydrogen exchange is performed using a spin column, to avoid dilution of the complex. Although this process is slower than the more typical 10-fold dilution into D_2O buffer, it is an important choice for hydrogen exchange studies of complexes so that dilution does not lead to dissociation of the complex during the exchange time course. After each desired exchange time, an aliquot of the sample is removed and the exchange is quenched at pH 2.5 and 0 °C. Finally, each exchanged sample is applied to another spin column to exchange from a buffer that supports assembly of a functional complex to a volatile buffer compatible with mass spectrometry. Each sample is immediately flash-frozen in liquid nitrogen and stored at −80 °C until mass spectrometry analysis.

Kinase assays were used to identify conditions that maximize the fraction of receptor in functional complexes. Because CheA in active complexes with chemoreceptors has 200-fold greater kinase activity than CheA alone in solution,[31] maximal kinase

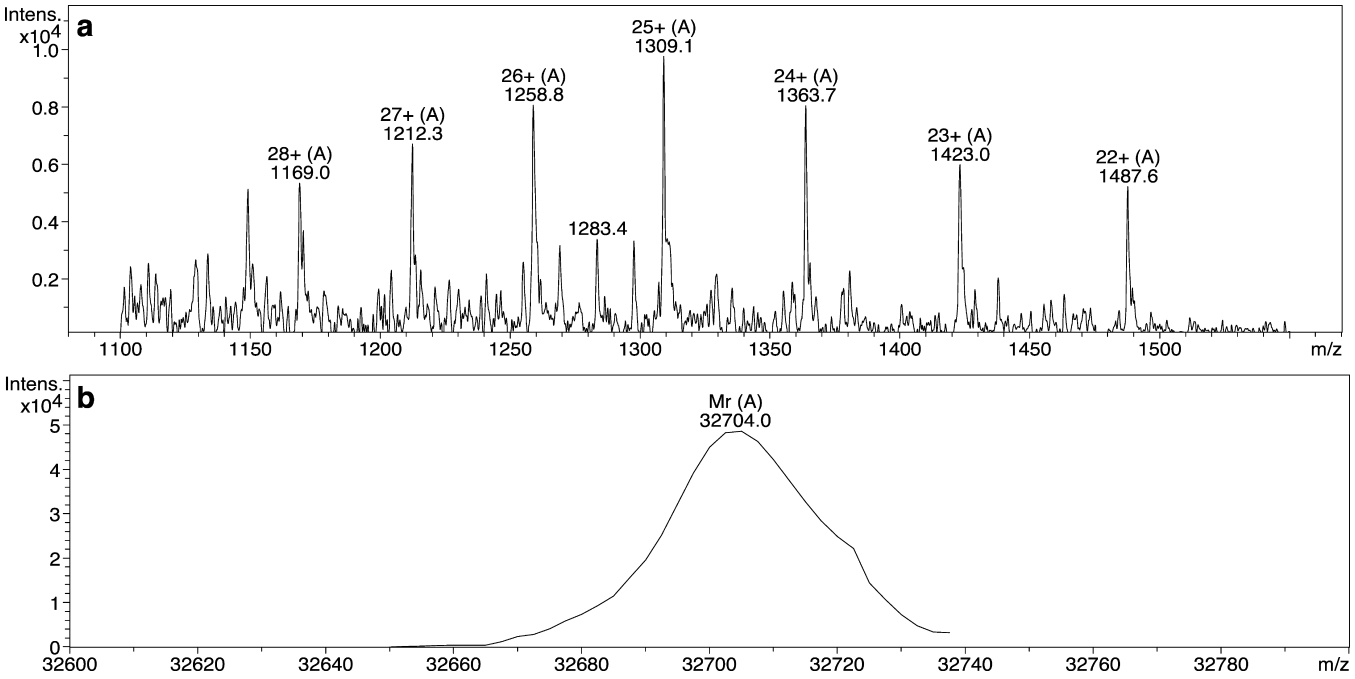

Figure 2. Mass spectrometry of the CF from functional complexes. (a) Mass spectrum showing the charge state distribution of CF_{4E} (+28 to +22 charge state peaks shown). (b) Deconvolution of the charge state distribution provides the average molecular mass of CF_{4E}. Note that although the signal:noise ratio is reduced in these samples that also contain vesicles and additional proteins, good mass accuracy and reproducibility are obtained. As reported in Table 2, the mass error estimated from independent measurements is ±3 Da.

activity indicates maximal complex formation. We chose conditions under which all the CF_{4E} is bound to vesicles (30 μM CF_{4E} and 580 μM lipid in extruded vesicles). In the presence of excess CheW (20 μM), kinase activity was measured as a function of CheA concentration and reached a maximum at 5 μM CheA (Figure S1a of the Supporting Information). Thus, we chose 6 μM CheA, as it was sufficient to drive maximal formation of active complexes. With the CheA concentration fixed at 6 μM, kinase activity was measured as a function of CheW concentration and reached a maximum at 10 μM CheW (Figure S1b of the Supporting Information). Therefore, 12 μM CheW and 6 μM CheA were chosen as conditions favoring maximal incorporation of 30 μM CF into vesicle-bound, kinase-activating complexes. A sedimentation assay (Figure S2 of the Supporting Information) confirms that all of the CF is bound to the vesicles. Comparison of the amounts of CheA and CheW present in the total and supernatant lanes indicates that some CheA and CheW are bound to the vesicle complexes (slightly greater amounts in the total lane), but a large excess remains in the supernatant. The use of excess CheA and CheW is consistent with the goal of having all of the CF_{4E} in complexes with these proteins.

Quenching at acidic pH dissociates the majority of the receptor cytoplasmic fragments from the vesicles, which facilitates mass spectral analysis. We hypothesized that quenching to pH 2.5 (which is needed to minimize further exchange) would protonate the His tag on CF_{4E}, causing dissociation of the complex from the vesicles. The results of a sedimentation assay indicate that 75% of the CF_{4E} does dissociate from the complex, based on the intensity of the CF_{4E} band in the postquench supernatant in Figure S2 of the Supporting Information. Moreover, we observed that these acidic conditions also lead to the precipitation of CheA and CheW, because their bands disappear from the postquench supernatant. This may reduce the amount of CheA and CheW injected into the MS instrument in subsequent steps (although the protocol does not involve a centrifugation step that would remove the precipitated proteins), which would be helpful for the current MS analysis of CF_{4E} but could hinder MS analysis of CheA and CheW in a future study.

Despite the complexity of the sample, clear ESI-MS data are obtained for CF_{4E} from functional complexes on vesicles with CheA and CheW. Figure 2 shows representative MS results, including (a) the charge state distribution and (b) the results of the deconvolution of these charge states to obtain the average molecular mass of CF_{4E}. The measured molecular mass of 32704 ± 3 Da is in excellent agreement with the calculated molecular mass of CF_{4E} of 32707 Da.

Control experiments were performed to measure the extent of amide backbone back exchange for this experimental protocol. After hydrogen to deuterium exchange is quenched, the buffer exchange (desalting spin column) introduces a protonated buffer, and then back exchange can occur during freezing, thawing, and injection into the ESI-MS. Two independent methods were used to determine the extent of back exchange. One approach measured the mass difference between samples that were buffer exchanged into a protonated versus deuterated MS buffer. This difference, which was the same for CF_{4E} alone and CF_{4E} in vesicle-bound complexes, represents the total number of deuterons that back exchange due to the buffer exchange into protonated MS buffer. The other approach measured the mass of the CF fully deuterated via thermal denaturation and renaturation in a deuterated buffer, followed by buffer exchange into the protonated MS buffer. The difference between this mass and the theoretical mass of deuterated CF_{4E} again represents the total number of deuterons that back exchange due to the steps conducted in protonated MS buffer. As shown in Table 1, these methods gave consistent values for total back exchanged protons. Assuming the back exchange includes all side chain sites, the calculated

dx.doi.org/10.1021/bi401261b | *Biochemistry* 2013, 52, 8833−8842

Table 1. Back Exchange for the Experimental Protocol

	buffer exchange with H vs D buffer	denatured and refolded in D_2O
total no. of sites back exchanged	331 ± 3[a]	338 ± 2[b]
no. of backbone amide sites back exchanged[c] (% of 300 total)	331 − 302 = 29 (10%)	338 − 302 = 36 (12%)

[a]The mass after the D_2O desalting column minus the mass after the H_2O desalting column (mean ± standard deviation of two measurements). [b]The mass of the fully deuterated protein (calculated) minus the mass of the D_2O-denatured protein after the H_2O desalting column (mean ± standard deviation of two measurements). [c]Assuming all 302 side chain sites back exchange.

number of back exchanged backbone amide sites is 30−36. This relatively low extent of back exchange, 10−12% of the amide backbone sites, indicates that the protocol is well-optimized for rapid postquench handling of the pH 2.5, chilled samples (each sample is unfrozen for approximately 3 min between the quench and MS spectrum).

Global HDX-MS Demonstrates a Large-Scale Change in Receptor Dynamics upon the Formation of Functional Complexes. Using the protocol described above, global hydrogen exchange (exchange of amide protons of the entire protein) was measured for the Asp receptor CF_{4E} in solution and for CF_{4E} assembled in functional complexes with CheA and CheW on 50% DOPC/50% DGS-NTA-Ni^{2+} vesicles. Figure 3

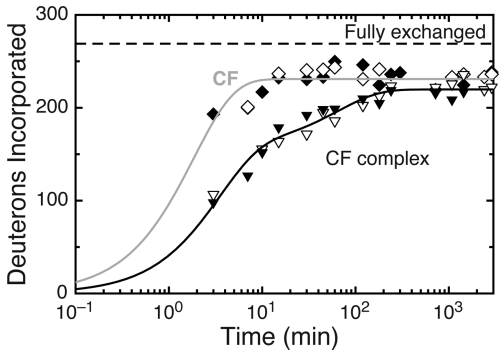

Figure 3. Global hydrogen exchange of CF_{4E}. Exchange occurs faster for the CF in solution (diamonds) than in functional complexes assembled at a high density on vesicles with CheA and CheW (triangles). Black and white symbols represent independent experiments. The estimated error of ±3 Da is smaller than the data symbols. The dashed line shows maximal possible exchange of 269 protons obtained for CF_{4E} denatured in D_2O (corrected for back exchange). Lines are monoexponential (gray) and biexponential (black) fits to the data.

shows that hydrogen exchange of CF_{4E} in functional complexes (triangles) is substantially slower than hydrogen exchange of CF_{4E} alone in solution (diamonds), with exchange behavior consistent for independent experiments (white vs black). The intermediate case, the CF bound to vesicles in the absence of CheA and CheW, was not investigated because previous studies have shown that such samples are prone to CF-mediated vesicle aggregation that interferes with formation of functional complexes.[41] The lines in Figure 3 represent monoexponential (gray) and biexponential (black) fits of the data for CF_{4E} in solution and CF_{4E} in functional complexes, respectively.

Table 2 compares the exchange rates and fractions for CF_{4E} in solution and CF_{4E} in kinase-on functional complexes. In both cases, there is a very fast fraction (f_0) that back exchanges too quickly to be monitored by the experiment, estimated to be 32 amide protons (11%) based on controls described above. There is also a very slow fraction (f_3) of 37−42 protons (12−14%) that do not exchange in 16 h. This was previously observed for the CF in solution: in deuterium exchange NMR[24] or tritium exchange[45] experiments, approximately 10% of CF_{2Q2E} does not exchange even after long times (3 days). The measured exchange time course for the CF in solution shows a single fast exchange phase for all 231 remaining protons, with a rate constant of 0.54 min^{-1}. In contrast, for the CF in functional complexes, nearly a third of these protons (71 protons) exhibit a 50-fold slower exchange rate of 0.01 min^{-1}, and a biexponential curve that includes "fast" and "slow" exchange rates is needed to achieve an adequate fit. A further slowing of hydrogen exchange for the CF in complexes results in a fast exchange rate that is reduced from 0.54 to 0.37 min^{-1}. A single isotopic cluster was observed in the mass spectra at each exchange time, consistent with a single population of the CF rather than a fast exchanging (heavy) and slow exchanging (light) population. This indicates that the biphasic behavior is due to different exchange rates for protons within each structural region of CF rather than different conformations of the CF. The overall change for the CF upon formation of functional complexes is from a protein with nearly all (90%) fast exchanging amide protons to one with only ∼60% fast exchanging protons.

Receptor Signaling States Do Not Exhibit Large-Scale Changes in Dynamics. For intact chemotaxis receptors, ligand binding to the periplasmic domain and methylation of the cytoplasmic domain (at the green sites shown in Figure 1A) shift the signaling state in opposite directions between the kinase-on/methylation-off state (favored by methylation) and the kinase-off/methylation-on state (favored by attractant ligand binding). Although the CF lacks the ligand binding domain of the receptor, different methylation state constructs can be compared to investigate differences between signaling states. Furthermore, Weis and co-workers demonstrated that complexes of CF_{4E}, CheA, and CheW assembled on vesicles at high and low density (50 and 10% nickel-chelating lipid, respectively) exhibit kinase-on/methylation-off and kinase-off/methylation-on activities, respectively.[33] These activity measurements suggested that CF_{4E} assembled in functional complexes on vesicles at low density (10% nickel-chelating lipid) mimics the ligand-bound signaling state of the intact receptor, and all other preparations (CF_{4E} at high density and CF_{4Q} at low or high density) mimic the ligand-free signaling state.

Table 2. Hydrogen Exchange Rates for CF_{4E} in Solution and in Functional Complexes

	f_0 (very fast)[a]	f_1 (fast)	k_1 (min^{-1})	f_2 (slow)	k_2 (min^{-1})	f_3 (very slow)[a]
cytoplasmic fragment[b]	32 ± 3 (11%)	231 ± 2 (77%)	0.54 ± 0.06	0	0	37 (12%)
kinase-active complex[c]	32 ± 3 (11%)	155 ± 6 (51%)	0.37 ± 0.05	71 ± 6 (24%)	0.01 ± 0.04	42 (14%)

[a]f_0 based on back exchange controls (average of three measurements); errors in other parameters are errors of the fit. f_3 is the remainder to reach 300 amide protons. [b]Fit to $y = f_1 - f_1e^{k_1t}$. [c]Fit to $y = f_1 + f_2 - (f_1e^{k_1t} + f_2e^{k_2t})e^{k_1t}$.

dx.doi.org/10.1021/bi401261b | Biochemistry 2013, 52, 8833−8842

Therefore, comparisons of hydrogen exchange of high-density complexes (50% nickel-chelating lipid) of CF_{4E} and CF_{4Q} investigate the effect of methylation, and comparisons of high- and low-density complexes of CF_{4E} investigate the effect of signaling state.

Close inspection of Figure 4 and Table 3 reveals no significant differences in measured global hydrogen exchange for high-density complexes of CF_{4Q}, high-density complexes of CF_{4E}, or low-density complexes of CF_{4E}. Any differences between the exchange of different states are no greater than the difference between replicates of the high-density CF_{4E} state (white triangles with a dashed line and black triangles with a black line in Figure 4). This is also clear in the fit parameters listed in Table 3, which are all largely within the range found for the replicates of the high-density CF_{4E} state. Therefore, we conclude that there are no significant differences measurable by global hydrogen exchange between these signaling states of functional CF complexes.

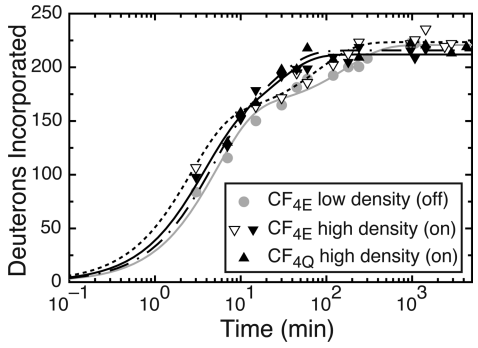

Figure 4. Global hydrogen exchange of CF complexes in different signaling states. The kinase-off state (gray circles and line) is prepared by assembly of CF_{4E} at low density (10% nickel-chelating lipid). The kinase-on state is prepared by either assembly of CF_{4E} at high density (50% nickel-chelating lipid, black and white inverted triangles, which are the same data as shown in Figure 3, fit by black and dashed lines, respectively) or assembly of CF_{4Q} at high density (black upward-pointing triangles and dashed−dotted line). The estimated error of ±3 Da is smaller than the symbols.

Local Exchange Measurements Are Feasible in Functional Complexes. Local exchange measurements, which involve analysis of exchange properties of individual peptides derived from the complex, would make it possible to determine if there are small-scale changes in hydrogen exchange and to localize those changes within the protein. Furthermore, proposals for the role of dynamics in chemoreceptor signaling suggest that increased dynamics in one region may be counterbalanced by decreased dynamics of another region,[34,35,48] which might not be detectable in a global exchange measurement unless the fast and slow exchange rates differed by at least 10-fold so they could be resolved by the global exchange experiment. Therefore, we developed a local exchange protocol for template-assembled functional complexes (see Figure 1B), involving a pepsin digest to generate peptides that were identified by tandem MS (MS/MS). As for the global exchange experiment, a series of exchanged samples were prepared and frozen for later MS analysis. In this case, samples were flash-frozen immediately after hydrogen exchange had been quenched. However, sample thawing was very slow and resulted in protein aggregation, both of which were resolved by modifying the quench buffer to 1% formic acid, 1 M GuHCl, and 20% glycerol (pH 1.6). This prevented protein aggregation and decreased the thawing time to 3 min.

The peptide map shown in Figure S3 of the Supporting Information displays the peptic peptides identified by tandem MS. The same peptides, which cover 84% of the sequence of this construct, were observed following pepsin digestion of CF_{4E} both in solution and in vesicle-bound complexes, in the original potassium phosphate quench buffer and in the modified GuHCl buffer. MS/MS analysis to identify the peptides was performed in guanidine hydrochloride (GuHCl) buffer. The CF sequence begins at residue 257, after the N-terminal His tag sequence, resulting in a coverage of the actual CF sequence of 87%. A CF sample denatured in D_2O was used as a control to determine the extent of back exchange for each peptide under the HDX protocol. As shown in Table S1 of the Supporting Information, the CF peptides exhibited between 13 and 30% back exchange, with an average back exchange of 20%. The 87% peptide coverage and 20% average back exchange indicate that local exchange measurements should be possible for this and other template-assembled complexes. These measurements are underway and, while beyond the scope of this work, will be the subject of a future publication.

DISCUSSION

By combining vesicle template assembly with HDX-MS measurements, we have measured global exchange of chemoreceptor cytoplasmic fragments in functional signaling complexes to resolve a paradox regarding the dynamics of this receptor domain. The HDX-MS results for exchange of the CF alone in solution, 88% fast and 12% very slow, are consistent with previous experiments using NMR or tritium exchange, which revealed 90% exchange in <15 min and a 10% core that does not exchange in 3 days.[24,45] The dynamic nature of the cytoplasmic domain seemed to be incompatible with transmission of a subtle ∼2 Å piston motion, so measuring the dynamics in a functional complex was critical to understanding the mechanistic details of the chemoreceptor signaling mechanism. Our results show that exchange rates of the CF are significantly slowed in functional complexes, suggesting this domain is less dynamic, which is more compatible with signaling via tiny conformational changes. Furthermore, there are no large-scale changes in exchange between signaling states,

Table 3. Hydrogen Exchange Rates for CF Complexes in Different Signaling States[a]

	f_1	k_1 (min^{-1})	f_2	k_2 (min^{-1})	f_3 (very slow)[b]
CF_{4E} at low density (kinase-off state) (●)	160 ± 7	0.20 ± 0.02	60 ± 8	0.006 ± 0.002	48
CF_{4E} at high density (kinase-on state) (▽)	154 ± 6	0.37 ± 0.05	71 ± 6	0.012 ± 0.003	43
CF_{4E} at high density (kinase-on state) (▼)	133 ± 23	0.31 ± 0.08	79 ± 22	0.042 ± 0.015	56
CF_{4Q} at high density (kinase-on state) (▲)	134 ± 41	0.25 ± 0.12	81 ± 41	0.049 ± 0.02	53

[a]Reported errors are errors of the fitting. Errors are substantially greater, as estimated from averaging the two replicate samples of CF_{4E} at high density to yield a k_2 of 0.027 ± 0.021. [b]Assuming f_0 = 32 back exchanged amide protons, f_3 is the remainder to reach 300 amide protons.

dx.doi.org/10.1021/bi401261b | Biochemistry 2013, 52, 8833−8842

which is again consistent with there being only subtle conformational differences between these states.

The CF in solution is α-helical, elongated, typically monomeric, and highly dynamic:[24] it most likely forms a fluctuating coiled-coil structure. The crystal structure of the CF alone and in complexes shows that it dimerizes into a four-helix bundle,[49,50] as independently predicted by extensive cysteine scanning studies of the cytoplasmic domain of the intact receptor.[51] Table 4 compares the exchange properties of CF_{4E} to those of two proteins with similar structures, a coiled coil (GCN4)[52] and a four-helix bundle (acyl coenzyme A binding protein, ACBP).[53] CF_{4E} in solution exhibits much faster exchange (~90% fast and 10% slow) than GCN4 and ACBP (~40% fast and 60% slow), consistent with our previous conclusion that the CF has a fluctuating tertiary structure,[24] and with the conclusion of disulfide scanning studies that this domain is a dynamic four-helix bundle.[27] The hydrogen exchange rates of CF_{4E} in functional complexes (~60% fast and 40% slow) are more consistent with those of GCN4 and ACBP. Thus, the CF in functional vesicle-bound complexes exhibits hydrogen exchange properties similar to those of stable proteins with similar structural motifs. This behavior of the CF is reminiscent of that of some intrinsically disordered proteins that form stable structures only upon binding to their protein partners.[54]

Table 4. Hydrogen Exchange Rates for the CF Compared to Those of Similar Protein Structures[a]

	method	$f_0 + f_1$ (fast)	$f_2 + f_3$ (slow)
GCN4 (coiled coil)[52]	NMR	~43%, $k > 0.1$ min^{-1}	~57%, k from 0.08 to 0.0005 min^{-1}
ACBP (four-helix bundle)[53]	NMR	~36%, $k > 0.1$ min^{-1}	~64%, k from 0.08 to 0.0002 min^{-1}
Asp receptor cytoplasmic fragment (CF)	MS	88%, $k \geq 0.5$ min^{-1}	12%, $k \leq$ 0.0001 min^{-1}
CF in a kinase-active complex	MS	62%, $k \geq 0.3$ min^{-1}	38%, k from 0.01 to $\leq$ 0.0001 min^{-1}

[a]Published rates corrected for differences in pH and temperature,[55] to pH 7.1 and 25 °C for comparison with CF data.

Large-scale reductions in the level of hydrogen exchange upon formation of protein−protein complexes have been reported in other systems. For example, binding of three different peptides to calmodulin reduces the global level of hydrogen exchange of the protein, and this reduction is thought to be due to stabilization of calmodulin. The global exchange rates show a change similar to that observed in CF complexes: the number of protons that exchange at the slowest rates of ~0.01 min^{-1} increases from zero in apocalmodulin to ~20 (18%) in the peptide-bound complexes.[56] Similarly, binding of the antitoxin IFS (immunity factor for SPN) to the bacterial toxin SPN (*Streptococcus pyogenes* NAD^+ hydrolase) reduces the level of exchange in both proteins. This reduced level of exchange is thought to be due to both decreased solvent accessibility at the SPN−/IFS protein interface and stabilization (increased level of hydrogen bonding) within each protein.[57]

Quantitative interpretation of the extent of protein stabilization corresponding to an observed change in the hydrogen exchange rate depends on the type of exchange. Hydrogen exchange in stable proteins is typically in the EX2 limit, where the rate-determining step is the intrinsic exchange rate (k_{int}).[10] In this limit, the measured exchange rate (k_{HDX}) depends on the fraction of time the amide site is in the open, exchange-competent conformation, given by the equilibrium constant for the opening event (K_{open}): $k_{HDX} = k_{int}K_{open}$. We can write the folding equilibrium constant as $K_{close} = 1/K_{open} = k_{int}/k_{HDX}$. CF complexes display EX2 exchange, but the CF in solution exchanges too quickly to determine whether exchange is in the EX1 or EX2 limit. If we assume that both exhibit EX2 exchange, then the ratio of the exchange rates can be used to estimate the magnitude of the stabilization upon formation of the complex. For the 71 residues that show substantial slowing of exchange upon formation of the complex, $K_{close}(\text{complex})/K_{close}(\text{CF}) = k_{HDX}(\text{CF})/k_{HDX}(\text{complex}) = 0.5\ \text{min}^{-1}/0.01\ \text{min}^{-1} = 54$, and a net estimated stabilization of the "closed" state by a $\Delta\Delta G$ of 2.4 kcal/mol.

We have also shown that local hydrogen exchange measurements on template-assembled complexes are feasible, by incorporating a pepsin digest step, using tandem MS to identify peptides that cover 87% of the CF sequence, and demonstrating that only 20% amide backbone back exchange occurs for these peptides (on average) with our protocol. HDX-MS measurements of local exchange will be important in the chemoreceptor system to identify which CF regions are stabilized in functional complexes and to determine if there are differences in exchange between signaling states. Specific models have been proposed for changes in dynamics of the cytoplasmic domain between signaling states based on mutagenesis and cysteine cross-linking data.[34,35] These models propose localized compensatory changes (increased dynamics in one region and decreased dynamics in another region) that would not have been detected by our global exchange measurements. Local hydrogen exchange measurements using the method we have demonstrated provide a promising approach for direct measurements of dynamics throughout the CF in different signaling states.

Here we have developed and demonstrated an HDX-MS method for monitoring dynamics and conformational changes of proteins in functional membrane-bound complexes. Applications of HDX-MS to monitor dynamics have recently expanded to include membrane proteins in detergent micelles[18−22] and in nanodiscs.[58] Our method for HDX-MS of functional complexes assembled on vesicles provides a complementary approach that will be important for systems, such as chemoreceptor arrays, that are not stable in detergent and are too large for nanodiscs. Cytoplasmic domains of other membrane proteins such as receptor kinases can be assembled into functional complexes with vesicle template assembly[36−39] for both global and local HDX-MS measurements. This tool is a promising approach for gaining insights into the structure and functional dynamics of membrane proteins.

■ ASSOCIATED CONTENT

Supporting Information

Activity measurements identifying conditions for maximal complex formation (Figure S1), gels demonstrating binding and release of components from vesicles (Figure S2), map of peptides identified by MS/MS (Figure S3), back exchange values for peptides identified by MS/MS (Table S1), and detailed methods for protein purification, assembly of functional complexes, and the strategy used for peptide identification. This material is available free of charge via the Internet at http://pubs.acs.org.

AUTHOR INFORMATION

Corresponding Author

*Department of Chemistry, 122 LGRT, 710 N. Pleasant St., University of Massachusetts, Amherst, MA 01003. E-mail: thompson@chem.umass.edu. Telephone: (413) 545-0827.

Funding

This research was supported by National Institutes of Health Grant R01-GM085288. S.S.K. was partially supported by a fellowship from the University of Massachusetts as part of the Chemistry-Biology Interface Training Program (National Research Service Award T32 GM08515).

Notes

The authors declare no competing financial interest.
[‖]Deceased.

ACKNOWLEDGMENTS

We thank Dr. Daniel Fowler, Dr. Fe Sferdean, Dr. Michael Harris, and Dr. Sandy Parkinson for helpful discussions and extend special thanks to Dr. Daniel Fowler and Yuzhou Tang for providing CheW and CheA proteins.

DEDICATION

This paper is dedicated to the memory of our colleague and friend, Bob Weis.

ABBREVIATIONS

CF, cytoplasmic fragment of the *Escherichia coli* aspartate chemotaxis receptor; DEAE, diethylaminoethanol; DGS-NTA, 1,2-dioleoyl-*sn*-glycero-3-[*N*-(5-amino-1-carboxypentyl)]-iminodiacetic acid (Ni-chelating lipid); DMSO, dimethyl sulfoxide; DOPC, 1,2-dioleoyl-*sn*-glycero-3-phosphocholine; GuHCl, guanidine hydrochloride; HDX-MS, hydrogen–deuterium exchange mass spectrometry; HPLC, high-pressure liquid chromatography; LC–ESI-MS, liquid chromatography and electrospray ionization mass spectrometry.

REFERENCES

(1) Boehr, D. D., McElheny, D., Dyson, H. J., and Wright, P. E. (2006) The Dynamic Energy Landscape of Dihydrofolate Reductase Catalysis. *Science 313*, 1638–1642.

(2) Nygaard, R., Zou, Y., Dror, R. O., Mildorf, T. J., Arlow, D. H., Manglik, A., Pan, A. C., Liu, C. W., Fung, J. J., Bokoch, M. P., Thian, F. S., Kobilka, T. S., Shaw, D. E., Mueller, L., Prosser, R. S., and Kobilka, B. K. (2013) The Dynamic Process of β_2-Adrenergic Receptor Activation. *Cell 152*, 532–542.

(3) Liu, J. J., Horst, R., Katritch, V., Stevens, R. C., and Wüthrich, K. (2012) Biased Signaling Pathways in β2-Adrenergic Receptor Characterized by ^{19}F-NMR. *Science 335*, 1106–1110.

(4) Kofuku, Y., Ueda, T., Okude, J., Shiraishi, Y., Kondo, K., Maeda, M., Tsujishita, H., and Shimada, I. (2012) Efficacy of the β_2-adrenergic receptor is determined by conformational equilibrium in the transmembrane region. *Nat. Commun. 3*, 1045.

(5) Loo, R. R., Dales, N., and Andrews, P. C. (1996) The effect of detergents on proteins analyzed by electrospray ionization. *Methods Mol. Biol. 61*, 141–160.

(6) Funk, J., Li, X., and Franz, T. (2005) Threshold values for detergents in protein and peptide samples for mass spectrometry. *Rapid Commun. Mass Spectrom. 19*, 2986–2988.

(7) Rundlett, K. L., and Armstrong, D. W. (1996) Mechanism of signal suppression by anionic surfactants in capillary electrophoresis-electrospray ionization mass spectrometry. *Anal. Chem. 68*, 3493–3497.

(8) Barrera, N. P., and Robinson, C. V. (2011) Advances in the mass spectrometry of membrane proteins: From individual proteins to intact complexes. *Annu. Rev. Biochem. 80*, 247–271.

(9) Morgner, N., Montenegro, F., Barrera, N. P., and Robinson, C. V. (2012) Mass spectrometry: From peripheral proteins to membrane motors. *J. Mol. Biol. 423*, 1–13.

(10) Eyles, S. J., and Kaltashov, I. A. (2004) Methods to study protein dynamics and folding by mass spectrometry. *Methods 34*, 88–99.

(11) Marcsisin, S. R., and Engen, J. R. (2010) Hydrogen exchange mass spectrometry: What is it and what can it tell us? *Anal. Bioanal. Chem. 397*, 967–972.

(12) Konermann, L., Pan, J., and Liu, Y.-H. (2011) Hydrogen exchange mass spectrometry for studying protein structure and dynamics. *Chem. Soc. Rev. 40*, 1224–1234.

(13) Yamamoto, T. (2004) Mass Spectrometry of Hydrogen/Deuterium Exchange of *Escherichia coli* Dihydrofolate Reductase: Effects of Loop Mutations. *J. Biochem. 135*, 487–494.

(14) Zhang, J., Chalmers, M. J., Stayrook, K. R., Burris, L. L., Garcia-Ordonez, R. D., Pascal, B. D., Burris, T. P., Dodge, J. A., and Griffin, P. R. (2010) Hydrogen/deuterium exchange reveals distinct agonist/partial agonist receptor dynamics within vitamin D receptor/retinoid X receptor heterodimer. *Structure 18*, 1332–1341.

(15) Zhang, H.-M., Yu, X., Greig, M. J., Gajiwala, K. S., Wu, J. C., Diehl, W., Lunney, E. A., Emmett, M. R., and Marshall, A. G. (2010) Drug binding and resistance mechanism of KIT tyrosine kinase revealed by hydrogen/deuterium exchange FTICR mass spectrometry. *Protein Sci. 19*, 703–715.

(16) Zhou, B., and Zhang, Z.-Y. (2007) Application of hydrogen/deuterium exchange mass spectrometry to study protein tyrosine phosphatase dynamics, ligand binding, and substrate specificity. *Methods 42*, 227–233.

(17) Tsutsui, Y., Dela Cruz, R., and Wintrode, P. L. (2012) Folding mechanism of the metastable serpin α1-antitrypsin. *Proc. Natl. Acad. Sci. U.S.A. 109*, 4467–4472.

(18) Orban, T., Jastrzebska, B., Gupta, S., Wang, B., Miyagi, M., Chance, M. R., and Palczewski, K. (2012) Conformational dynamics of activation for the pentameric complex of dimeric G protein-coupled receptor and heterotrimeric G protein. *Structure 20*, 826–840.

(19) West, G. M., Chien, E. Y. T., Katritch, V., Gatchalian, J., Chalmers, M. J., Stevens, R. C., and Griffin, P. R. (2011) Ligand-dependent perturbation of the conformational ensemble for the GPCR β2 adrenergic receptor revealed by HDX. *Structure 19*, 1424–1432.

(20) Chung, K. Y., Rasmussen, S. G. F., Liu, T., Li, S., DeVree, B. T., Chae, P. S., Calinski, D., Kobilka, B. K., Woods, V. L., and Sunahara, R. K. (2011) Conformational changes in the G protein Gs induced by the β2 adrenergic receptor. *Nature 477*, 611–615.

(21) Rey, M., Man, P., Clémençon, B., Trézéguet, V., Brandolin, G., Forest, E., and Pelosi, L. (2010) Conformational dynamics of the bovine mitochondrial ADP/ATP carrier isoform 1 revealed by hydrogen/deuterium exchange coupled to mass spectrometry. *J. Biol. Chem. 285*, 34981–34990.

(22) Mehmood, S., Domene, C., Forest, E., and Jault, J.-M. (2012) Dynamics of a bacterial multidrug ABC transporter in the inward- and outward-facing conformations. *Proc. Natl. Acad. Sci. U.S.A. 109*, 10832–10836.

(23) Hebling, C. M., Morgan, C. R., Stafford, D. W., Jorgenson, J. W., Rand, K. D., and Engen, J. R. (2010) Conformational analysis of membrane proteins in phospholipid bilayer nanodiscs by hydrogen exchange mass spectrometry. *Anal. Chem. 82*, 5415–5419.

(24) Seeley, S. K., Weis, R. M., and Thompson, L. K. (1996) The cytoplasmic fragment of the aspartate receptor displays globally dynamic behavior. *Biochemistry 35*, 5199–5206.

(25) Danielson, M. A., Bass, R. B., and Falke, J. J. (1997) Cysteine and disulfide scanning reveals a regulatory α-helix in the cytoplasmic domain of the aspartate receptor. *J. Biol. Chem. 272*, 32878–32888.

(26) Chervitz, S. A., and Falke, J. J. (1996) Molecular mechanism of transmembrane signaling by the aspartate receptor: A model. *Proc. Natl. Acad. Sci. U.S.A. 93*, 2545–2550.

(27) Winston, S. E., Mehan, R., and Falke, J. J. (2005) Evidence that the Adaptation Region of the Aspartate Receptor Is a Dynamic Four-Helix Bundle: Cysteine and Disulfide Scanning Studies. *Biochemistry 44*, 12655−12666.
(28) Maddock, J. R., and Shapiro, L. (1993) Polar location of the chemoreceptor complex in the *Escherichia coli* cell. *Science 259*, 1717−1723.
(29) Briegel, A., Ortega, D. R., Tocheva, E. I., Wuichet, K., Li, Z., Chen, S., Müller, A., Iancu, C. V., Murphy, G. E., Dobro, M. J., Zhulin, I. B., and Jensen, G. J. (2009) Universal architecture of bacterial chemoreceptor arrays. *Proc. Natl. Acad. Sci. U.S.A. 106*, 17181−17186.
(30) Zhang, P., Khursigara, C. M., Hartnell, L. M., and Subramaniam, S. (2007) Direct visualization of *Escherichia coli* chemotaxis receptor arrays using cryo-electron microscopy. *Proc. Natl. Acad. Sci. U.S.A. 104*, 3777−3781.
(31) Shrout, A. L., Montefusco, D. J., and Weis, R. M. (2003) Template-Directed Assembly of Receptor Signaling Complexes. *Biochemistry 42*, 13379−13385.
(32) Montefusco, D. J., Asinas, A. E., and Weis, R. M. (2007) Liposome-mediated assembly of receptor signaling complexes. *Methods Enzymol. 423*, 267−298.
(33) Besschetnova, T. Y., Montefusco, D. J., Asinas, A. E., Shrout, A. L., Antommattei, F. M., and Weis, R. M. (2008) Receptor density balances signal stimulation and attenuation in membrane-assembled complexes of bacterial chemotaxis signaling proteins. *Proc. Natl. Acad. Sci. U.S.A. 105*, 12289−12294.
(34) Swain, K. E., Gonzalez, M. A., and Falke, J. J. (2009) Engineered Socket Study of Signaling through a Four-Helix Bundle: Evidence for a Yin−Yang Mechanism in the Kinase Control Module of the Aspartate Receptor. *Biochemistry 48*, 9266−9277.
(35) Zhou, Q., Ames, P., and Parkinson, J. S. (2009) Mutational analyses of HAMP helices suggest a dynamic bundle model of input-output signalling in chemoreceptors. *Mol. Microbiol. 73*, 801−814.
(36) Zhang, X., Gureasko, J., Shen, K., Cole, P. A., and Kuriyan, J. (2006) An allosteric mechanism for activation of the kinase domain of epidermal growth factor receptor. *Cell 125*, 1137−1149.
(37) Shrout, A. L., Esposito, E. A., and Weis, R. M. (2008) Template-directed Assembly of Signaling Proteins: A Novel Drug Screening and Research Tool. *Chem. Biol. Drug Des. 71*, 278−281.
(38) Esposito, E. A., Shrout, A. L., and Weis, R. M. (2008) Template-Directed Self-Assembly Enhances RTK Catalytic Domain Function. *J. Biomol. Screening 13*, 810−816.
(39) Shi, F., Telesco, S. E., Liu, Y., Radhakrishnan, R., and Lemmon, M. A. (2010) ErbB3/HER3 intracellular domain is competent to bind ATP and catalyze autophosphorylation. *Proc. Natl. Acad. Sci. U.S.A. 107*, 7692−7697.
(40) Kott, L., Braswell, E. H., Shrout, A. L., and Weis, R. M. (2004) Distributed subunit interactions in CheA contribute to dimer stability: A sedimentation equilibrium study. *Biochim. Biophys. Acta 1696*, 131−140.
(41) Montefusco, D. J., Shrout, A. L., Besschetnova, T. Y., and Weis, R. M. (2007) Formation and Activity of Template-Assembled Receptor Signaling Complexes. *Langmuir 23*, 3280−3289.
(42) Fowler, D. J., Weis, R. M., and Thompson, L. K. (2010) Kinase-active Signaling Complexes of Bacterial Chemoreceptors Do Not Contain Proposed Receptor−Receptor Contacts Observed in Crystal Structures. *Biochemistry 49*, 1425−1434.
(43) Asinas, A. E., and Weis, R. M. (2006) Competitive and cooperative interactions in receptor signaling complexes. *J. Biol. Chem. 281*, 30512−30523.
(44) Wu, J., Long, D. G., and Weis, R. M. (1995) Reversible dissociation and unfolding of the *Escherichia coli* aspartate receptor cytoplasmic fragment. *Biochemistry 34*, 3056−3065.
(45) Murphy, O. J., Yi, X., Weis, R. M., and Thompson, L. K. (2001) Hydrogen Exchange Reveals a Stable and Expandable Core within the Aspartate Receptor Cytoplasmic Domain. *J. Biol. Chem. 276*, 43262−43269.
(46) Zhang, Z., and Smith, D. L. (1993) Determination of amide hydrogen exchange by mass spectrometry: A new tool for protein structure elucidation. *Protein Sci. 2*, 522−531.
(47) Fang, J., Rand, K. D., Beuning, P. J., and Engen, J. R. (2011) False EX1 signatures caused by sample carryover during HX MS analyses. *Int. J. Mass Spectrom. 302*, 19−25.
(48) Zhou, Q., Ames, P., and Parkinson, J. S. (2011) Biphasic control logic of HAMP domain signalling in the *Escherichia coli* serine chemoreceptor. *Mol. Microbiol. 80*, 596−611.
(49) Kim, K. K., Yokota, H., and Kim, S. H. (1999) Four-helical-bundle structure of the cytoplasmic domain of a serine chemotaxis receptor. *Nature 400*, 787−792.
(50) Briegel, A., Li, X., Bilwes, A. M., Hughes, K. T., Jensen, G. J., and Crane, B. R. (2012) Bacterial chemoreceptor arrays are hexagonally packed trimers of receptor dimers networked by rings of kinase and coupling proteins. *Proc. Natl. Acad. Sci. U.S.A. 109*, 3766−3771.
(51) Falke, J. J., and Kim, S. H. (2000) Structure of a conserved receptor domain that regulates kinase activity: The cytoplasmic domain of bacterial taxis receptors. *Curr. Opin. Struct. Biol. 10*, 462−469.
(52) Goodman, E. M., and Kim, P. S. (1991) Periodicity of amide proton exchange rates in a coiled-coil leucine zipper peptide. *Biochemistry 30*, 11615−11620.
(53) Kragelund, B. B., Knudsen, J., and Poulsen, F. M. (1995) Local perturbations by ligand binding of hydrogen deuterium exchange kinetics in a four-helix bundle protein, acyl coenzyme A binding protein (ACBP). *J. Mol. Biol. 250*, 695−706.
(54) Dyson, H. J., and Wright, P. E. (2005) Intrinsically unstructured proteins and their functions. *Nat. Rev. Mol. Cell Biol. 6*, 197−208.
(55) Bai, Y., Milne, J. S., Mayne, L., and Englander, S. W. (1993) Primary structure effects on peptide group hydrogen exchange. *Proteins 17*, 75−86.
(56) Sperry, J. B., Huang, R. Y.-C., Zhu, M. M., Rempel, D. L., and Gross, M. L. (2011) Hydrophobic Peptides Affect Binding of Calmodulin and Ca as Explored by H/D Amide Exchange and Mass Spectrometry. *Int. J. Mass Spectrom. 302*, 85−92.
(57) Sperry, J. B., Smith, C. L., Caparon, M. G., Ellenberger, T., and Gross, M. L. (2011) Mapping the protein-protein interface between a toxin and its cognate antitoxin from the bacterial pathogen *Streptococcus pyogenes*. *Biochemistry 50*, 4038−4045.
(58) Morgan, C. R., Hebling, C. M., Rand, K. D., Stafford, D. W., Jorgenson, J. W., and Engen, J. R. (2011) Conformational transitions in the membrane scaffold protein of phospholipid bilayer nanodiscs. *Mol. Cell. Proteomics 10*, M111-010876.